Journal of Geophysical Research: Oceans

RESEARCH ARTICLE
10.1029/2017JC013623

Anticyclonic Eddy Edge Effects on Phytoplankton Communities and Particle Export in the Northern South China Sea

Lei Wang[1,2], Bangqin Huang[1], Edward A. Laws[3], Kuanbo Zhou[1], Xin Liu[1], Yuyuan Xie[1], and Minhan Dai[1]

[1]State Key Laboratory of Marine Environmental Science, Fujian Provincial Key Laboratory of Coastal Ecology and Environmental Studies, Xiamen University, Xiamen, China, [2]Third Institute of Oceanography, State Oceanic Administration, Xiamen, China, [3]Department of Environmental Sciences, College of the Coast and Environment, Louisiana State University, Baton Rouge, LA, USA

Key Points:
- The phytoplankton community composition had similarity among different anticyclonic eddies
- Eddies edge effect was obvious and discrepant for different phytoplankton groups
- The *physical-nutrients-phytoplankton-POC flux* dynamic process reflected both the vertical and horizontal inside/outside the eddies

Supporting Information:
- Supporting Information S1
- Data Set S1
- Data Set S2
- Data Set S3

Correspondence to:
B. Huang,
bqhuang@xmu.edu.cn

Citation:
Wang, L., Huang, B., Laws, E. A., Zhou, K., Liu, X., Xie, Y., & Dai, M. (2018). Anticyclonic eddy edge effects on phytoplankton communities and particle export in the northern South China Sea. *Journal of Geophysical Research: Oceans, 123*. https://doi.org/10.1029/2017JC013623

Received 8 NOV 2017
Accepted 24 AUG 2018
Accepted article online 4 SEP 2018

Abstract We examined response of phytoplankton total chlorophyll *a* (TChl *a*) and community composition to three coherent anticyclonic eddies (ACEs) observed during a cruise to the northern South China Sea on 28 July to 7 August 2007. Photosynthetic pigments were measured to estimate the contribution of nine phytoplankton groups to TChl *a*. Although the water column-integrated TChl *a* inventory in the upper 100 m was very similar among the three ACEs (17.6–18.9 mg/m^2) we observed during the cruise, there were remarkable enhancements in biomasses at the eddy edges. TChl *a* inventory was 20.8 ± 3.0 mg/m^2 at the edge, which was 33% or 60% higher than at the center and reference. The greatest enhancement of the TChl *a* at edge was attributed to haptophyte-8, which was 1.6 and 2.2 times the analogous concentrations at the center and reference sites. The *Prochlorococcus* Chl *a* was ~50% greater at the edge relative to the reference and was intermediate at the center. Diatom Chl *a* at the edge was ~2.5 times the concentrations at the center and reference sites. The positive correlation between particulate organic carbon flux and haptophyte-8 Chl *a* at the edge implied an important role of haptophyte-8 in particle export productivity. It is interesting to note that there occurred higher fluxes of biogenic Si at the center of the ACEs due likely to lateral transport of diatoms from the edge. The phenomenon of higher TChl *a* at the edge but higher export at the center may have been the combined result of vertical convection and lateral transport within the eddies.

Plain Language Summary The response of different phytoplankton groups to three anticyclonic eddies (ACEs) and the relationship between the carbon export and phytoplankton community was studied in the northern South China Sea on July 28-August 7, 2007. The phytoplankton TChl a concentration inventory in the upper 100 m was very similar among the three ACEs. But the biomass and community composition varied in different parts of the ACEs, including the ACEs' centers, edges and outside the ACEs. The enhancement of TChl a at edge attributed to haptophyte-8 was siginificantly.The Prochlorococcus Chl a was ~50% greater at the edge relative to the reference and was intermediate at the center. The haptophyte-8 played an important role of in particle export. The phenomenon of higher TChl a at the edge but higher export at the center may have been the combined result of vertical convection and lateral transport within the eddies

1. Introduction

Mesoscale eddies are ubiquitous oceanic features that extend spatially over distances of tens to hundreds of kilometers and temporally over times of days to months (Chelton et al., 2011; Zhang et al., 2013). Eddies are classified into cyclonic eddies, anticyclonic eddies (ACEs), and mode-water eddies (McGillicuddy et al., 1999, 2007).

Numerous studies have shown that mesoscale eddies play an important role in biogeochemical cycles initiated by their effects on nutrient dynamics in the euphotic zone (Klein & Lapeyre, 2009; Martin & Pondaven, 2003; Nurser & Zhang, 2000). It has been estimated that 20–40% of the nutrient requirements of phytoplankton are supplied by mesoscale eddies (Mahadevan & Archer, 2000; McGillicuddy et al., 2003; Oschlies & Garçon, 1998). Nitrogen fixation and submesoscale processes can provide allochthonous nutrients for new production (Glover et al., 2008; Kolber, 2006; Lévy et al., 2001; McGillicuddy et al., 2007; Moore et al., 2007). Nutrient pumping induces an enhancement of phytoplankton biomass, community

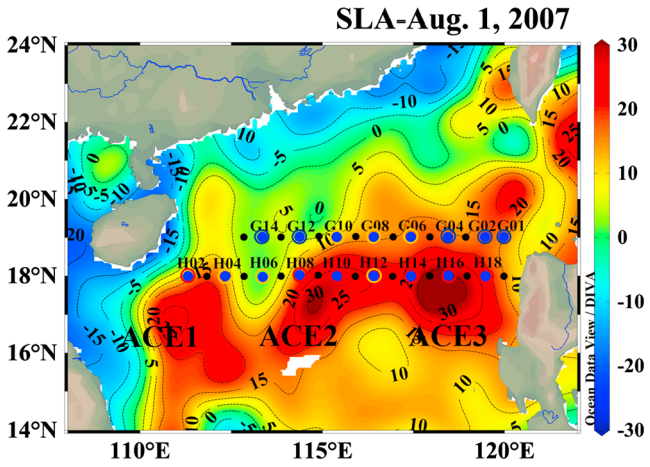

Figure 1. Map of sampling stations based on the sea level anomaly on 1 August 2007. The blue dots were stations with phytoplankton pigment survey in all 33 stations during the cruise. The three anticyclonic eddies were named ACE1, ACE2, and ACE3 from the west to the east along transect H. The red, yellow, and blue cycles on the station dots indicate the center, edge, and reference stations of the ACEs, respectively. ACES = anticyclonic eddies; SLA = sea level anomaly.

succession, and primary production, especially in the oligotrophic subtropical ocean (Eden & Dietze, 2009; Landry et al., 2008; Lévy et al., 2009; MacFadyen et al., 2008; McGillicuddy et al., 2007; Oguz & Salihoglu, 2000; Painter et al., 2010). These effects are easily explained in the case of a cyclonic eddy based on the doming of its isopycnals and nutricline. The mechanism is more complicated in the case of an ACE. Because of the depression of its isopycnals, there is not obvious nutrient pumping in the ACE center, and the absence of a biological response has been reported in many ACE studies (Biggs, 1992; Leterme & Pingree, 2008; Sweeney et al., 2003; Tanaka et al., 2011). However, positive effects on phytoplankton biomass and primary production have been reported in some ACEs. The postulated mechanisms have included (1) the importation of shelf waters or terrigenous nutrients (Campbell et al., 2013; Dietze et al., 2009; Hansen et al., 2010; Moore et al., 2007; Paterson et al., 2008; Perissinotto & Rae, 1990; Washburn et al., 1993); (2) Ekman pumping induced by wind stress (José et al., 2014; Martin & Richards, 2001; Woodward & Rees, 2001; Zhang et al., 2001); (3) nitrogen fixation (Fong et al., 2008; Guidi et al., 2012); (4) the rebound of depressed isopycnals and the release of nutrients during the decay stage of the ACE (Crawford et al., 2007; Flierl & Mied, 1985; Franks et al., 1986; Nelson et al., 1989; Tranter et al., 1980); and (5) the enhancement of particle sinking as a result of the *wineglass shape* structure of the ACE (Waite et al., 2016) and during the spring bloom in the North Atlantic (Omand et al., 2015). In recent studies, a scenario involving the perimeter of an ACE or eddy-eddy interactions has been discussed. This mechanism may be another explanation for the stimulation of biological production observed in some ACEs (Guidi et al., 2012; Jeffrey & Hallegraeff, 1980; Kim et al., 2012; Kishi, 1994; Omand et al., 2015; Peterson et al., 2011; Toner et al., 2003).

Mesoscale eddies occur frequently in the South China Sea (SCS), which has facilitated studies of their impacts on biogeochemical cycles. In the case of ACEs, almost all the biomass-modulating mechanisms have been reported in at least one study, including the lack of a response or a reduction in biomass (Huang et al., 2010; Ning et al., 2004, 2008) and enhancement by importation of shelf water (Lin et al., 2010) or by eddy advection (Liu et al., 2013). Even though a physical-biogeochemical model indicates that new production is reduced by one third in ACEs compared to the mean value in the SCS basin (Xiu & Chai, 2011), enhancement of Chl *a* in the filament structure and the resulting enhancement of carbon export have been reported at the perimeter of ACEs in the SCS (Liu et al., 2013; Sasai et al., 2013; Zhou et al., 2013). Based on fieldwork carried out on the same cruise as this study, Zhou et al. (2013) have addressed submesoscale variability associated with ACEs and their effects on particle export at the submesoscale. In this study, the details of the response of phytoplankton TChl *a* concentrations and community composition to these three ACEs will be expatiated.

2. Data and Methods

2.1. Cruise and Sample Collection

The cruise was carried out in the northern SCS basin with the R/V *Dongfanghong 2* from 28 July to 7 August 2007 (Figure 1). Samples were collected along two transects from 111.5°E to 120°E based on the sea level anomaly: Transect H along 18°N and Transect G along 19°N. The locations of the three ACEs were identified using the sea level anomaly acquired from the French Archiving, Validation, and Interpolation of Satellite Oceanographic data project (Nan et al., 2011; Zhou et al., 2013). Transect H extended through three ACEs —ACE1, ACE2, and ACE3—from west to east (Figure 1).

A conductivity-temperature-depth (CTD) system (SeaBird SBE-911 Plus, Bellevue, WA, USA) was deployed to acquire hydrographic parameters. Seawater samples for phytoplankton pigment analysis using high-performance liquid chromatography (HPLC) were collected at five depths (0, 25, 50, 75, and 100 m) with CTD-mounted rosette assemblies and 12-L Niskin bottles (General Oceanics, Inc., Miami, FL, USA).

2.2. HPLC Pigments

Seawater samples (6–16 L) for phytoplankton pigment analyses were filtered onto 47-mm Whatman GF/F filters under gentle vacuum (<120 mm Hg). The filters were wrapped with aluminum foil, frozen, and stored in liquid nitrogen on board the research vessel. The frozen samples were later placed in a freezer (−80 °C) after transportation to the laboratory. Pigments were extracted with 2 mL of N,N-dimethylformamide in a freezer (−20 °C) for 2 h (Furuya et al., 1998). The extracts were then filtered through 13-mm Whatman GF/F filters in a Swinnex filter holder to remove filter debris before mixing with 1 mol/L ammonium acetate solution (600 μL:600 μL). Subsamples were injected into an HPLC system (Agilent series 1100, Santa Clara, CA, USA) equipped with a 3.5-μm Eclipse XDB C_8 column (100 × 4.6 mm; Agilent Technologies) following the elution protocol described by Zapata et al. (2000). The quantification was confirmed using standards purchased from the Danish Hydraulic Institute Water and Environment, Hørsholm, Denmark. Six chlorophylls and 12 xanthophylls could be quantified. The chlorophylls included monovinyl chlorophyll *a*, divinyl chlorophyll *a*, monovinyl chlorophyll *b,* divinyl chlorophyll *b,* chlorophyll c_1 + c_2, and chlorophyll c_3. The xanthophylls included alloxanthin, 19′-butanoyloxyfucoxanthin, diadinoxanthin, diatoxanthin, fucoxanthin, 19′-hexanoyloxyfucoxanthin, lutein, neoxanthin, peridinin, prasinoxanthin, violaxanthin, and zeaxanthin.

2.3. Phytoplankton Community Composition

The chemical taxonomy program CHEMTAX V1.0 was used to estimate the contribution of different phytoplankton groups to the TChl *a* concentration (Mackey et al., 1996). Thirteen pigments were used to quantify the fraction of the TChl *a* contributed by each of nine phytoplankton groups—dinoflagellates, diatoms, haptophyte-8, haptophyte-6, chlorophytes, cryptophytes, *Prochlorococcus*, *Synechococcus*, and prasinophytes. The initial matrix of pigment/Chl *a* ratios followed the protocol used by Mackey et al. (1996). Residual analysis indicated that the pigment/Chl *a* ratios had converged by the fifth iteration of CHEMTAX (Latasa, 2007).

Based on more detailed pigment information, Zapata et al. (2004) divided haptophytes into eight pigment types by analyzing 37 species (65 strains) of haptophytes (Zapata et al., 2004). The main differences between the haptophyte-6 and haptophyte-8 were the relatively small concentrations of 19′-but-fucoxanthin in type-6 versus type-8, and the opposite pattern for Mv-Chl c_3. *Emiliania huxleyi* and *Gephyrocapsa oceanica* belong to haptophyte-6, whereas species like *Dicrateria inornata*, *Imantonia rotunda*, and *Phaeocystis* belong to haptophyte-8.

2.4. Particle Export Data

The data for particulate organic carbon (POC) concentrations, thorium-234 (^{234}Th) fluxes, ^{234}Th/^{238}U, POC fluxes, and biogenic SiO_2 ($bSiO_2$) concentrations have been reported in Zhou et al. (2013).

2.5. Data Analysis

Pearson's correlation coefficient was used to identify the correlations between two variables. Independent *t* tests combined with one-way analysis of variance were used to compare the difference between two groups. All the statistical analyses were carried out with OriginPro v8.5 (OriginLab Corporation©, Northampton, MA, USA). Ocean Data View software (v4.6.1) was used to plot the contour figures.

3. Results

3.1. Hydrochemical Structure

The sea level anomaly images identified the location of the three ACEs during the 2007 cruise (Figure 1 & Figure S1). According to the study of Nan et al. (2011), the centers of the three eddies were located at 111.7°E, 17.7°N for ACE1; 115.0°E, 17.9°N for ACE2; and 118.1°E, 17.5°N for ACE3 on 22 August 2007, respectively. It was obvious that the positions of the three ACEs were stable during the 3 weeks of our survey, except for the position of ACE2, which moved northward by a few kilometers. Based on the standard of 5 cm contours in altimetry (Hwang & Chen, 2000), the diameters of the three ACEs (150 km, 156 km, and 178 km for ACEs 1, 2, and 3, respectively) reported by Nan et al. (2011) were also stable during the 3 weeks. ACE1, ACE2, and ACE3 were all long-lived and lasted 147 days, 168 days, and 210 days, respectively (Nan et al., 2011). From the beginning of our survey, their lifetimes were 74 days, 67 days, and 56 days, respectively.

Table 1
The Hydrologic Parameters of the Three Station Types (Center, Edge, and Reference) in the Three Anticyclone Eddies (ACEs)

Types	ACEs	Station	SST (°C)	SSS	MLD (m)	θ = 23.5 kg/m^3 depth (m)
Center	1	H02	30.24	33.74	23.0	75.0
	2	H08, H10	30.58	33.70	22.5	82.5
	3	H14, H16, H18	30.92 ± 0.20	33.69 ± 0.07	20.0 ± 3.6	88.3 ± 3.3
	Average	n = 6	30.70 ± 0.69	33.70 ± 0.06^b	21.3 ± 3.9^a	84.2 ± 5.4
Edge	1	H04	30.51	34.11	27.0	69.0
	2	H06, H12, G10	30.62 ± 0.31	33.83 ± 0.08	12.0 ± 2.2	76.3 ± 14.4
	3	G06, G08	30.57	33.88	13.5	69.5
	Average	n = 6	30.58 ± 0.24	33.90 ± 0.15^{ab}	15.8 ± 6.0^b	73.2 ± 11.8
Reference		G01, G02, G04, G12, G14	30.74 ± 0.26	34.04 ± 0.07^a	27.4 ± 5.8^a	75.6 ± 10.4

Note. The parameters included sea surface temperature (SST), sea surface salinity (SSS), the mixed layer depth (MLD), and the depth of the 23.5 kg/m^3 isopycnal. The reference group was treated as the control in the multiple comparison using one-way ANOVA. The superscript labels ^{a,b} and ^{ab} implied significant difference at the level of $p < 0.050$. ANOVA = analysis of variance.

The stations in the three ACEs (nine in Transect H and eight in Transect G) were categorized based on the temperature-salinity properties of the water and cluster analysis. The categories were the center, edge, and reference (stations outside the eddies; Table 1 and Figure 2; and Zhou et al. (2013)). The vertical distribution of temperature (T), salinity (S), and potential density anomaly (σ_0) along Transect H (Figures 3a–3c) and Transect G (Figures 3d–3f) during the 2007 cruise implied that all three ACEs had lower salinity (<33.7) in the surface water at the center. But there were no significant differences between the temperatures and σ_0 values in the surface water of the center, edge, and reference stations. The isohalines were typically depressed in the center. The S = 33.9 contour, for example, was at ~50 m at the center and at ~25 m at the edge. The isohalines at the edges of ACE1 and ACE2 domed dramatically; the S = 33.9 and S = 34.5 contours were ~50-m shallower than at the centers. Along Transect G, the isohalines and isopycnals at the reference stations were at depths intermediate between the shallower isohalines and isopycnals at the centers of the eddies and the deeper ones at the edges.

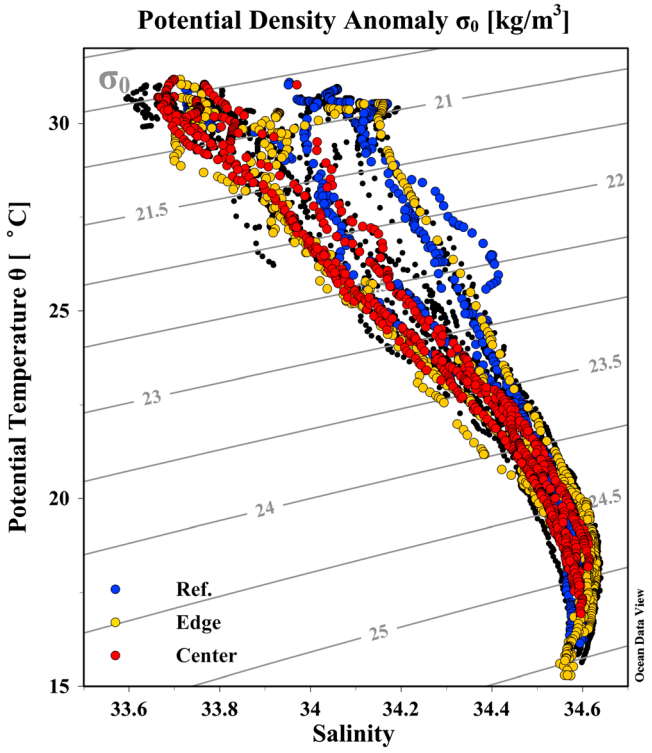

Figure 2. Potential temperature (θ) versus salinity scatters (T-S properties) showing the water mass in the upper 150-m water column for the August 2007 cruise. The dots represent potential density anomaly σ_0 (kg/m^3), and gray lines are the isopycnals. The center, edge, and reference stations were in red, yellow, and blue, respectively.

The distributions of dissolved inorganic nitrogen (DIN) and silicate [Si $(OH)_4$] along Transects H and G during the 2007 cruise have been shown in Zhou et al. (2013). Briefly, DIN was depleted in the upper 50 m along both zonal transects, but the Si $(OH)_4$ distribution was stratified. The nutricline was at ~75 m at the center of ACE1 and deeper (100 m) at the center of ACE2. The DIN was exhausted in the upper 100 m at the center of ACE3, and the nutricline was deeper than 100 m. However, the nutricline had a dramatic dome structure at the edges of the ACEs. At a depth of 100 m, for example, the DIN concentrations at the edges were 7–12 μmol/L compared to 0–6 μmol/L at the centers.

3.2. Phytoplankton TChl *a* Concentration

3.2.1. Vertical Distribution

The vertical distribution of TChl *a* concentrations along Transect H showed that the depth of the deep chlorophyll maximum layer (DCML) was stable at 75–100 m (Figure 4a). The concentration of TChl *a* varied from 0.228 to 0.546 mg/m^3 in the DCML along Transect H; the minimum value in the entire survey area was 0.147 mg/m^3 at station G02. There was no significant difference between the TChl *a* concentrations in the DCML among the three ACEs, but the TChl *a* concentration was distinctly higher ($p < 0.010$) at the edge (0.415 ± 0.081 mg/m^3) than at the center (0.284 ± 0.037 mg/m^3) or the reference (0.259 ± 0.085 mg/m^3). The

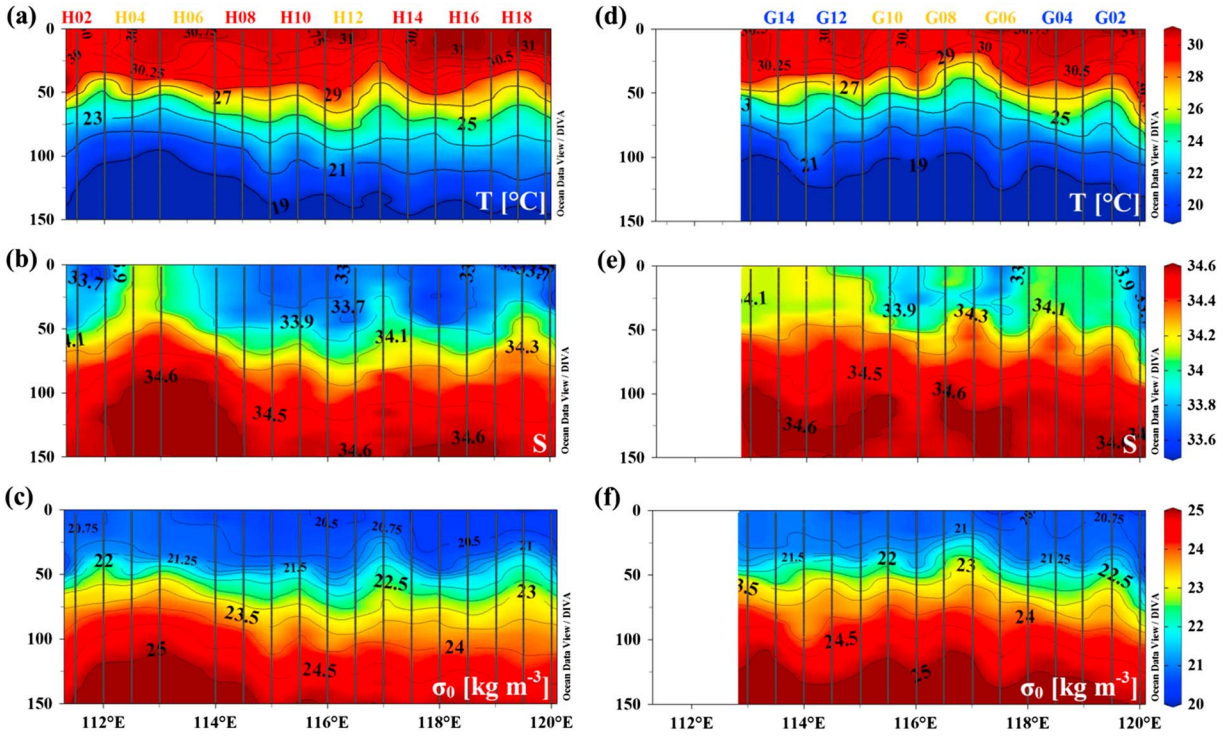

Figure 3. Vertical distribution of (a and d) temperature (°C), (b and e) salinity, and (c and f) potential density anomaly (σ_0, kg/m^3) in Transects H (left panel) and G (right panel) during the August 2007 cruise. The red, yellow, and blue on the station labels indicate the center, edge, and reference stations of the ACEs, respectively. ACES = anticyclonic eddies.

distributions of the phytoplankton groups were similar in the DCML and in the upper water column, except for *Synechococcus* (Figure 4f), which was present throughout the euphotic zone but was most numerous in the DCML (>0.040 mg/m^3). The haptophyte-8 group was dominant at the DCML and contributed ~50% to the TChl *a* concentration in that area (Figure 4c), followed by *Prochlorococcus*, which accounted for 20–25% of the phytoplankton TChl *a* concentration (Figure 4e). Approximately 10% of the TChl *a* concentration was contributed by *Synechococcus* (Figure 4f), similar to the haptophyte-6 contribution (Figure 4d). The Chl *a* concentration of diatoms was very low, only 3–7% (Figure 4b). The variations of the Chl *a* concentrations among the center, edge, and reference differed among phytoplankton groups. Almost all the phytoplankton groups were enhanced at the center and/or edge compared to the reference. The most dramatic elevation was the abundance of the predominant group, haptophyte-8, which was ~50% greater at the edge compared to the reference ($p < 0.050$). Although diatoms contributed very little to the TChl *a* concentration, they made an obviously greater contribution to the TChl *a* concentration at the edge, 5.4-fold higher compared to their contribution at both the center and reference ($p < 0.010$). *Prochlorococcus* and *Synechococcus* also showed a ~20% increase at the edge and center compared to the reference ($p < 0.050$).

3.2.2. Horizontal Comparison

The integrated TChl *a* concentration in the upper 100 m of the water column inventory was used to quantify the phytoplankton biomass (Figure 5). The TChl *a* inventories were 18.9 ± 1.2, 18.6 ± 4.0, and 17.6 ± 3.8 mg/m^2 for the ACE1, ACE2, and ACE3, respectively, which were approximately 40% higher than at the reference ($p < 0.010$), while there were no significant differences between the TChl *a* inventories as well as between the contribution of each phytoplankton group in the three eddies ($p > 0.050$). The predominant groups, the haptophyte-8 and *Prochlorococcus*, were elevated 80–90% ($p < 0.010$) and 30–40% ($p < 0.050$) in the ACEs compared to the reference. The Chl *a* concentrations of diatoms were almost the same at ACE3 and the reference, but they were 120% higher than the reference concentration at ACE1 and ACE2 ($p < 0.010$). The inventories of the *Synechococcus* Chl *a* concentrations were very similar between the ACEs and reference, although there was a 15% decrease at ACE1 ($p < 0.050$). Other

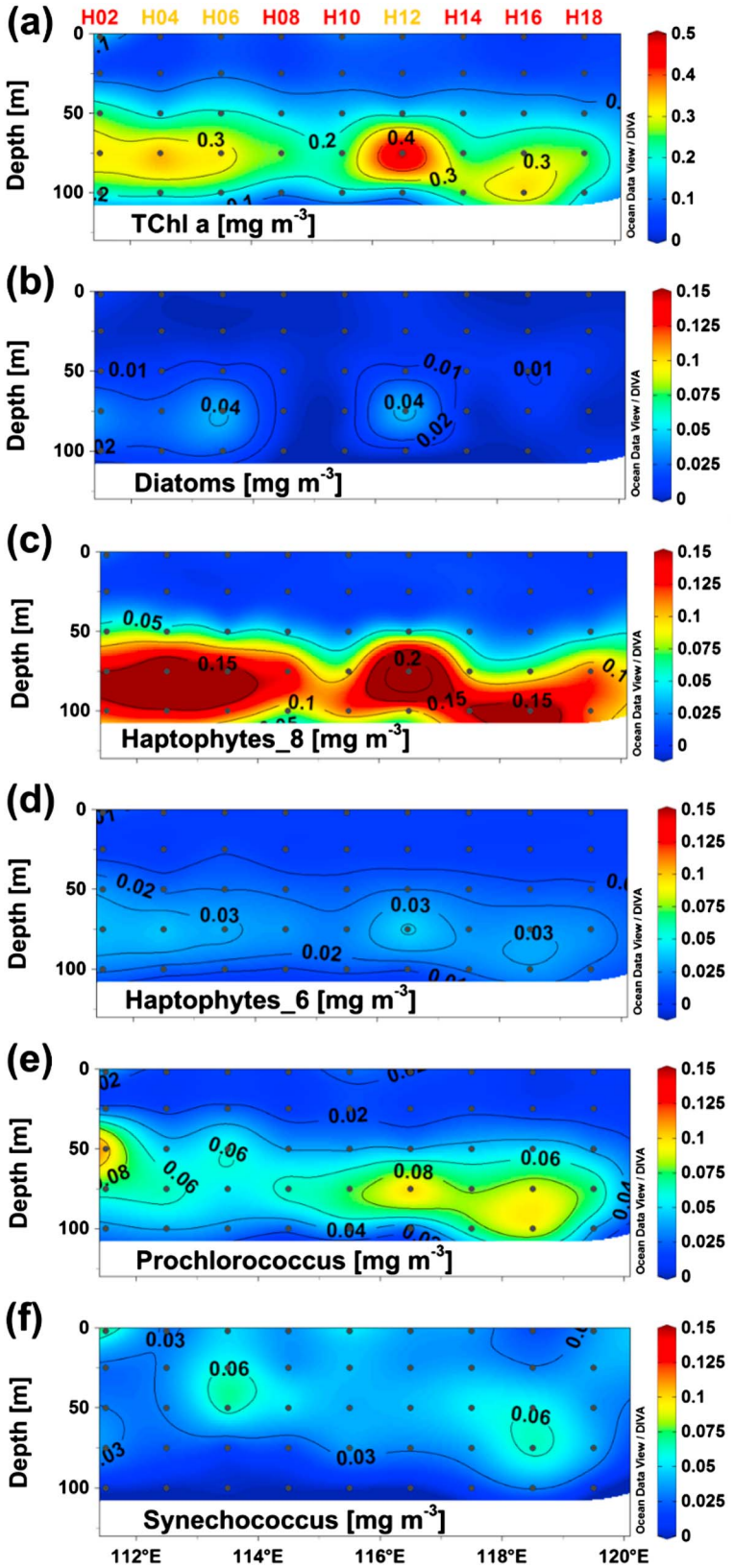

Figure 4. Vertical distribution of (a) TChl *a*, (b) diatoms, (c) haptophyte-8, (d) haptophyte-6, (e) *Prochlorococcus* and (f) *Synechococcus* TChl *a* concentration (mg/m^3) along transect H during the August 2007 cruise. The red, yellow, and blue on the station labels indicate the center, edge, and reference stations of the ACEs, respectively. ACES = anticyclonic eddies.

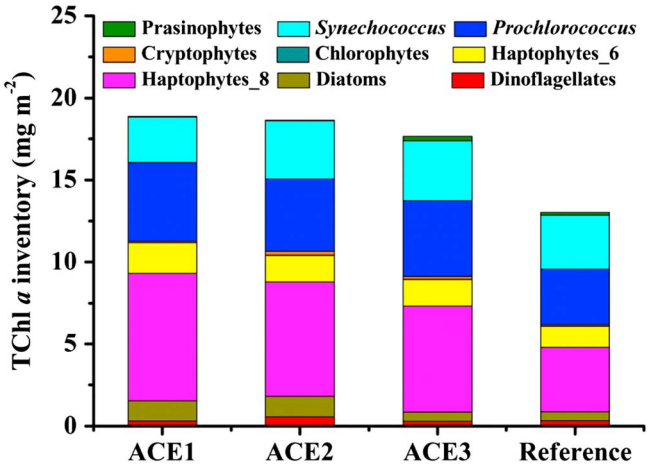

Figure 5. The contribution of phytoplankton groups to the upper 100-m TChl *a* inventory in the three ACEs and at the reference stations during the August 2007 cruise. ACES = anticyclonic eddies.

phytoplankton groups fluctuated simultaneously at the ACEs compared to the reference: a 25–45% increase for haptophyte-6 ($p < 0.050$), an ~80% decrease for prasinophytes ($p < 0.050$), and ~10% (variable) changes for dinoflagellates ($p > 0.050$).

3.2.3. Edge Effects

In order to address the effect of eddies on phytoplankton communities at the submesoscale, comparisons were made between the communities at the center, edge, and reference of the ACEs (Figure 6). There were distinct variations of the TChl *a* inventories and some of the dominant phytoplankton groups, especially at the edge. The TChl *a* inventory in the upper 100 m was 20.8 ± 3.0 mg/m^2 at the edge, which was higher by 33% ($p < 0.050$) and 60% ($p < 0.050$) compared to the center and reference, respectively (Figure 6a). The Chl *a* inventory of the haptophyte-8 group was enhanced the most at the edge, 60% higher than the inventory at the center ($p < 0.050$) and 120% higher than the inventory at the reference ($p < 0.050$, Figure 6d). The Chl *a* inventory of the second most abundant group, *Prochlorococcus*, was 50% greater at the edge relative to the reference ($p < 0.050$) and was intermediate at the center (Figure 6f). The pattern for haptophyte-6 was similar, about 40% enhancement at the edge relative to the reference (Figure 6e). *Synechococcus* was distributed homogeneously among the center, edge, and reference; the *Synechococcus* Chl *a* inventory varied from 3.32 ± 0.76 to 3.58 ± 0.47 mg/m^2 (Figure 6g). Although diatoms contributed only 3–7% to the TChl *a* inventory, the diatom Chl *a* inventory was 150% higher at the edge than at the center and the reference ($p < 0.050$, Figure 6c). The dinoflagellates (Figure 6b) and prasinophytes (Figure 6h) contributed only slightly to the TChl *a* inventory, and their Chl *a* inventories did not vary significantly. Their Chl *a* concentrations were elevated at the edge and somewhat variable.

3.3. Relationship Between the Phytoplankton Community and POC Flux

To elucidate the relationship between particle export and phytoplankton community composition, we classified the CHEMTAX-based phytoplankton groups into three size fractions: the microfraction (diatoms + dinoflagellates), the nano-fraction (haptophyte-8 + haptophyte-6 + chlorophytes + cryptophytes), and the pico-fraction (*Prochlorococcus* + *Synechococcus* + prasinophytes) in accord with (Uitz et al., 2006). Ternary graphs clearly showed that the contribution of the microfraction to TChl *a* was <25% in almost all the samples, and the major fluctuations occurred between the nano- and pico-fractions (Figure 7). The distribution patterns of TChl *a* (Figure 7a), POC (Figure 7b), and $bSiO_2$ (Figure 7d) were similar; the high values were principally at the eddy edges. The micro:nano:pico contribution was approximately 15:25:60. The distribution pattern of the $^{234}Th/^{238}U$ ratio (Th/U) was somewhat different (Figure 7c). The ratios were relatively high when the nanoplankton or picoplankton were most abundant and were relatively low when the distribution of size fractions was more balanced. At all sites the Th/U ratio was relatively high when the nanoplankton fraction was 60% more than the picoplankton fraction, independent of the absolute contribution.

To explain the distribution pattern of the Th/U ratio in relation to the phytoplankton size fractions, details of the vertical profiles for Th/U, TChl *a*, and the contributions of the major phytoplankton groups are shown in Figure 8. There were more deficits of Th/U in the upper 50 m of the water column at the center or edge than at the reference (Figures 8a–8c). The TChl *a* concentrations were also elevated at the center and edge relative to the reference (Figures 8d–8f). The deficits of Th/U in the upper 50 m were associated mainly with *Prochlorococcus* and *Synechococcus* (Figures 8g–8i). However, the pattern was more complicated at depths of 50–100 m, where the maximum Th/U deficits were 18.2% at 75 m at the center, 16.8% at 50 m at the edge, and 14.2% at 75 m at the reference. Remarkably, the ^{234}Th-^{238}U equilibrium was reestablished at 100 m at the edge, but there were still ~10% deficits at 100 m at the center and reference. This pattern might be explained by the profiles of the haptophyte-8 Chl *a* concentrations, which reached maxima of 0.128 mg/m^3 at the center and 0.133 mg/m^3 at the reference, both at a depth of 100 m. At the edge, the maximum haptophyte-8 Chl *a* concentration was 0.218 mg/m^3 at 75 m, and the haptophyte-8 Chl *a* concentration at 100 m was 0.119 mg/m^3, less than at the center and reference.

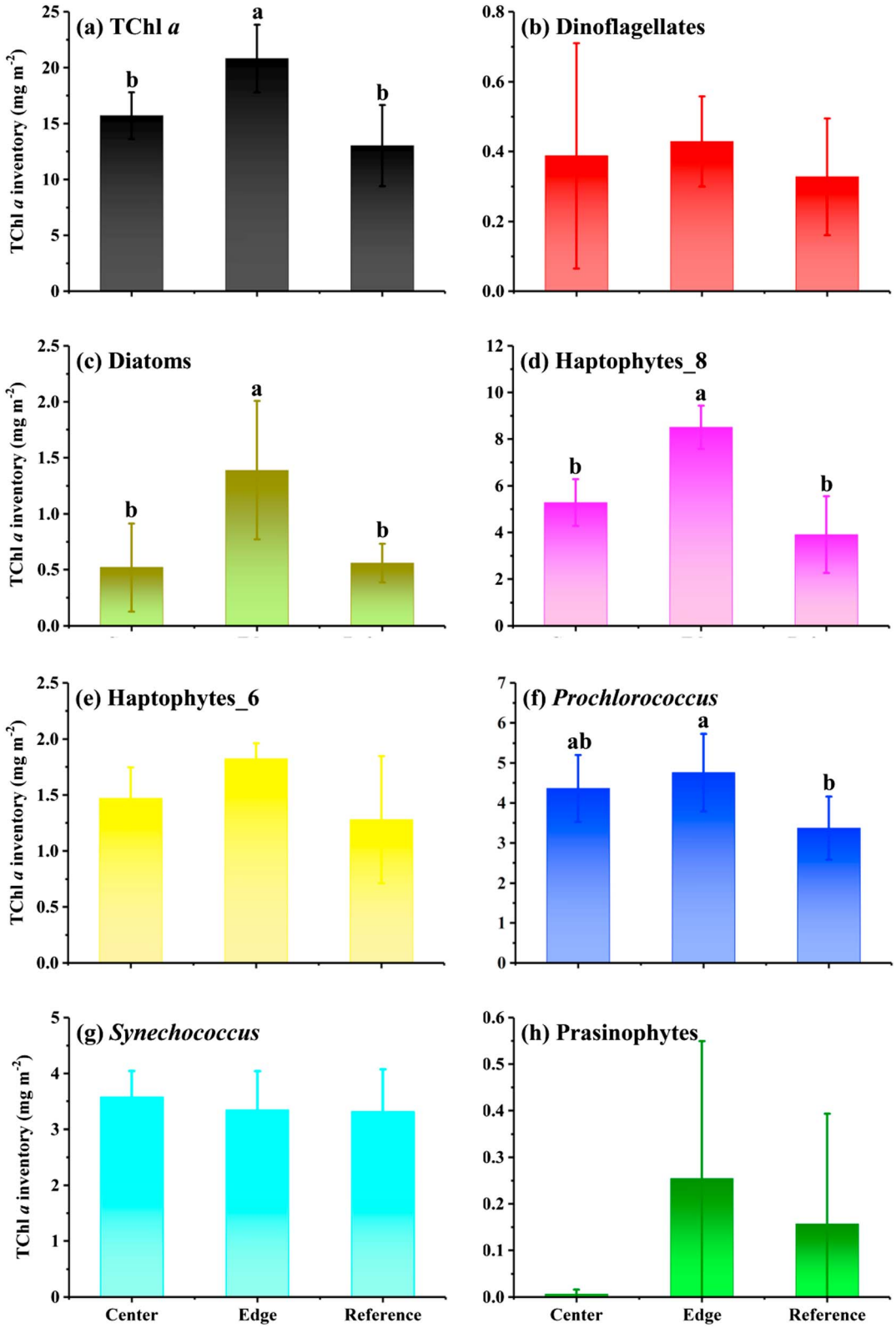

Figure 6. Post hoc multiple comparisons of (a) TChl *a*, (b) dinoflagellates, (c) diatoms, (d) haptophyte-8, (e) haptophyte-6, (f) *Prochlorococcus*, (g) *Synechococcus*, and (h) prasinophytes TChl *a* inventory (mg/m^2) in the upper 100-m water column between the ACEs' center, edge, and reference stations during the August 2007 cruise. The superscript labels ^{a}, ^{b}, and ^{ab} represent significant difference at the level of $p < 0.05$. ACES = anticyclonic eddies.

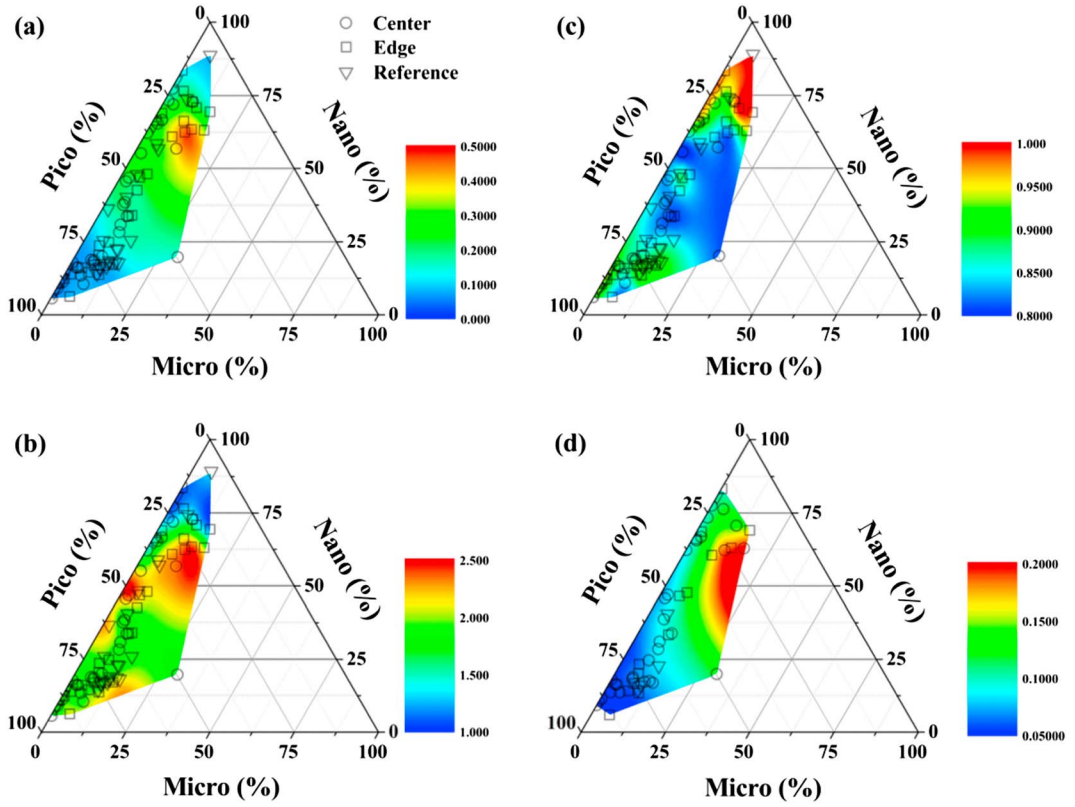

Figure 7. The ternary contours of (a) TChl *a* (mg/m^3), (b) particulate organic carbon (POC, mmol C/m^3), (c) ^{234}Th/^{238}U, and (d) biogenic SiO_2 ($bSiO_2$, mmol Si/m^3) based on the phytoplankton size fraction, including the microfraction, nano- and pico-fraction. The dots, squares, and inverted triangles represent the ACEs' center, edge, and reference stations, respectively. ACES = anticyclonic eddies.

4. Discussion

4.1. Modulation of the Phytoplankton TChl *a* Concentration at the ACE Edge

There were no obvious differences of phytoplankton TChl *a* concentrations and community compositions between the three ACEs, perhaps because their origins were within 3° of longitude and at similar stages from each other. The interiors of all three ACEs were located at bathymetries of 1,000 m, and all three ACEs could be defined as basin-scale ACEs (Nan et al., 2011). The similarity of their physical characteristics and their origins from the same current system could account for their similar phytoplankton distributions. ACE1 was generated from the western boundary current of the SCS 1 week before ACE2, which was generated from the eastward branch of the western boundary current along ~18°N. ACE3 was also generated from the same branch, but 3 weeks later than ACE2 (Nan et al., 2011). Thus, the lineal origins of the eddies and steady basin-scale circulation resulted in the three ACEs being slow moving and in synchrony.

The phytoplankton TChl *a* concentrations were elevated at the edges of all three ACEs, but this pattern is not universal among ACEs that are generated in eutrophic or oligotrophic water (Table 2). For example, the eddy Haida-2000a, which was generated off the coast of British Columbia, propagated westward and merged into the high-nitrate, low-chlorophyll waters of the Gulf of Alaska. Therefore, that ACE could trap typical coastal water at its center and develop higher Chl *a* concentration there than at its edge. Advective entrainment and upwelling resulted in the edges playing the role of a conduit between the eddy and the outside water, and the phytoplankton community therefore varied significantly (Peterson et al., 2011).

There have been other reports of similar scenarios, where the enhancement at the ACE's edge was obliterated at the center. These scenarios have been associated with ACEs that originate from the coast or shelf (Campbell et al., 2013; Jeffrey & Hallegraeff, 1980; Kim et al., 2012; Moore et al., 2007). The scenarios at the edges of ACEs that have been generated in typical oligotrophic oceanic environments have been similar

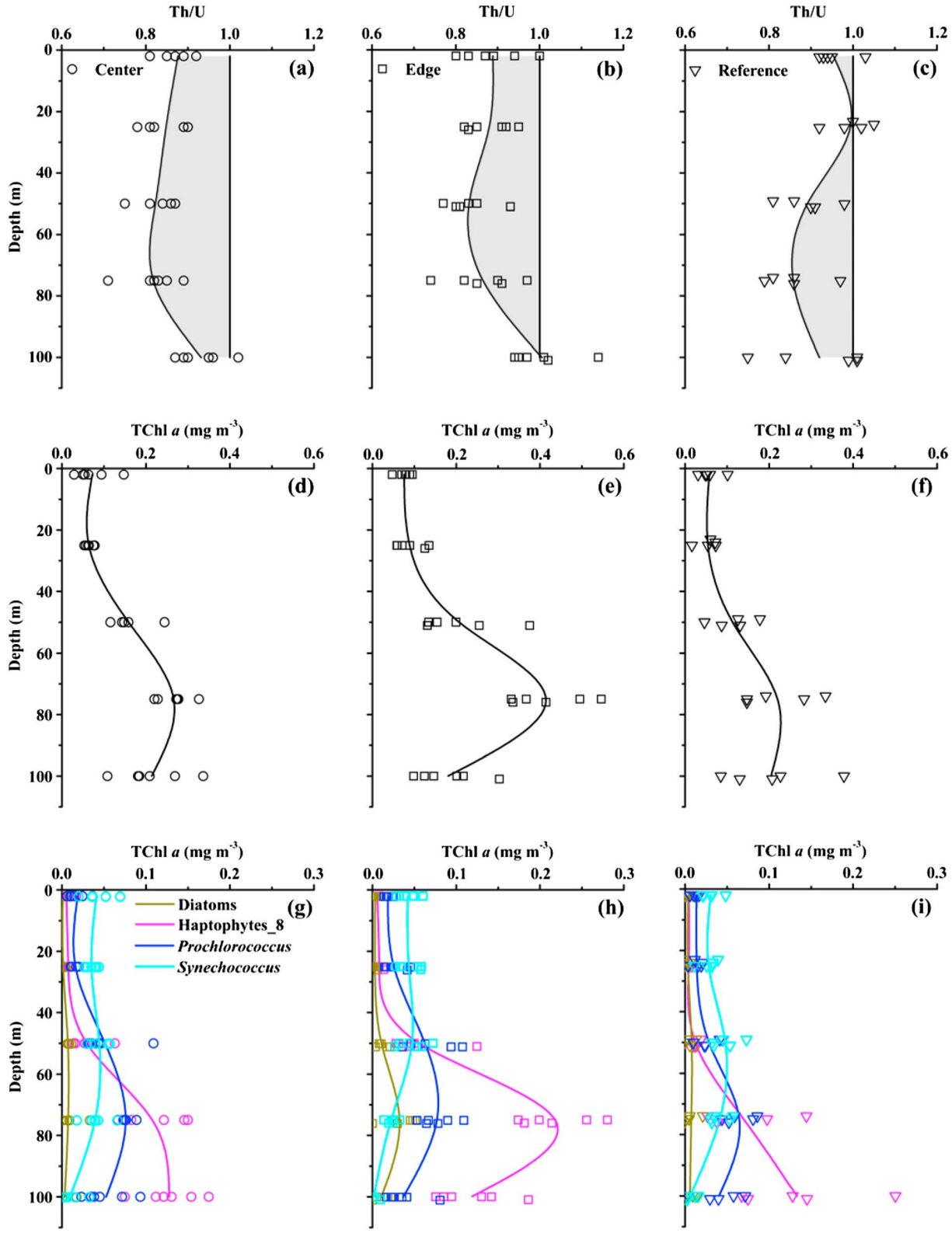

Figure 8. Vertical profiles of $^{234}Th/^{238}U$ (top panel, a–c), TChl *a* (mg/m^3) (middle panel, d–f), and TChl *a* concentration (mg/m^3) of the major four phytoplankton groups (bottom panel, g–i) in the upper 100 m for ACEs' center (dots, a, d, and g), edge (squares, b, e, and h), and reference stations (inverted triangles, c, f, and i). The gray shadow in Figures 8a–8c show the deficits of $^{234}Th/^{238}U$. All the splines represent the profiles of average values. The diatoms are in dark yellow, haptophyte-8 in magenta, *Prochlorococcus* in blue, and *Synechococcus* in cyan in Figures 8g–8i, respectively. ACES = anticyclonic eddies.

Table 2
Comparison of the Nutrient and Chl a Concentration Response Among the Center, Edge, and Reference in Various ACE Cases

Eddy name	Sea area	Time	Station types	DCML depth (m)	Inventory depth (m)	DIN @inventory (mmol/m^2)	Si $(OH)_4$ @inventory (mmol/m^2)	Chl *a* @DCML (mg/m^3)	Chl *a* @inventory (mg/m^2)	References
None	East Australian Current	Dec. 1978	Center	50–100	200	-	-	0.49–0.89	32.9–54.7	Jeffrey and Hallegraeff (1980)
			Edge	50–100	200	-	-	0.33–0.38	22.7–33.4	
			Reference	50–100	200	-	-	0.27–0.34	-	
None	Western Australian Coast	Sep. 2000	Center	-	250	-	-	0.06–0.15	48.8	Moore et al. (2007)
			Edge	-	250	-	-	0.10–0.27	49.6–51.8	
			Reference	-	250	-	-	0.10–0.20	20.2–24.5	
Haida-2000a	Gulf of Alaska	1 Jun. 2000–1 Sep. 2000	Center	54	50	261	457	0.67	24.5	Peterson et al. (2011)
			Edge	56	50	209	394	0.6	18.5	
			Reference	65	50	242	493	0.51	25	
Ulleung warm eddy	East Sea/ Japan Sea	Jul. 2005 Aug. 2007	Center	41	60	114	590	5.5	90.6	Kim et al. (2012)
			Edge	41	60	159	595	2.5	44.6	
			Reference	34	60	81	274	<1.0	20	
None	ALOHA	Aug. 2008	Center	-	-	81 ± 33	270 ± 23	0.4–0.6	-	Guidi et al. (2012)
			Edge	-	-	135 ± 10	374 ± 65	0.6–0.8	-	
$A1_{obs}A2_{obs}A3_{obs}$	Mozambique Channel	Apr. 2008 May 2009	Center	70–80	-	-	-	<0.10 0.25 0.30	-	José et al. (2014)
		Jan. 2004	Edge	50–80	-	-	-	0.10–0.30	-	
ACE1 ACE2 ACE3	northern SCS	Jul.-Aug. 2007	Center	83 ± 12	100	30 ± 37	332 ± 21	0.284 ± 0.037	15.712 ± 2.099	This study
			Edge	75 ± 1	100	228 ± 89	470 ± 113	0.415 ± 0.081	20.822 ± 3.026	
			Reference	90 ± 12	100	45 ± 49	312 ± 22	0.259 ± 0.085	13.022 ± 3.639	

Note. SCS = South China Sea; ACE = anticyclonic eddy; DCML = deep chlorophyll maximum layer DIN = dissolved inorganic nitrogen.

to our results to some extent, no matter whether the eddies were in a dipole- or single-ACE mode (Guidi et al., 2012; José et al., 2014). In the northern SCS, Liu et al. (2013) have attributed the elevation of Chl *a* at the edges of nonlinear ACEs to nutrient pumping. The west-to-east difference of Chl *a* concentrations along the periphery of the ACEs revealed a high-northeast and low-southeast pattern of Chl *a* concentrations in each ACE that seems consistent with our results (Liu et al., 2013).

4.2. Community Composition Under Edge Effects

In the present study, the Chl *a* inventory of most of the phytoplankton groups increased at the edge. The TChl *a* inventories at the edge were 30–60% greater than at the center or reference. The haptophyte-8 and diatoms were the most obvious components of the TChl *a* inventory that increased (Figure 6). The percentage of nano-phytoplankton biomass has been reported to increase from 45–59% at the center of an ACE to 72–76% at the edge (Table 3, Jeffrey & Hallegraeff, 1980). However, the major components of the eddy in the east Australian Current were prymnesiophytes (expressed as haptophyte-6 in this study), small dinoflagellates, and diatoms (<15 μm). The group described as haptophyceae was also the dominant component in the Haida-2000a eddy, but its biomass was higher at the center (58–62%) than at the edge (42–47%, Peterson, 2005). In the case of the ACE *WE2* in the northern SCS, the haptophyte-8 group was also the major contributor to the TChl *a* concentration (~35%) both inside and outside the eddy (Huang et al., 2010). In our study, if the reference was regarded as the background, then the haptophyte-8 group was responsible for 60% of the increase of the TChl *a* inventory at the edge, followed by 18% for *Prochlorococcus* and 11% for diatoms. This result implies that the enhancement of the haptophyte-8 group largely accounted for the elevation of the TChl *a* inventory stimulated by nutrient pumping at the edge.

The microphytoplankton, primarily diatoms and dinoflagellates, accounts for ~10% of primary production in the oligotrophic ocean, but their contribution to particle export reaches 65–70% through direct sinking or grazing (Michaels & Silver, 1988). In our study, although diatoms accounted for a minor percentage of the phytoplankton TChl *a* concentration, their 11% contribution to the enhanced biomass at the edge was still significant. According to Jeffrey and Hallegraeff (1980), there is a higher diversity of diatom species at an ACE edge than at the core, and the abundance of the large genus *Rhizosolenia* (45–69%) is higher than that of *Nitzschia* (1–21%) at the edge of the ACE; the contributions are roughly reversed at the center. This scenario

Journal of Geophysical Research: Oceans

10.1029/2017JC013623

Table 3
The Response of Phytoplankton Composition or Biomass Among the Center, Edge, and Reference to Various ACE Cases

Eddy name	Station types	Dino-	Diat-	Hapto-8	Hapto-6	Proc-	Syne-	Pras-	Micro (%)	Nano (%)	Pico (%)	References
None (▲)	Center	3×10^4	$>10^5$	-	9×10^4	-	-	4×10^5	-	45–59	-	Jeffrey and Hallegraeff (1980)
	Edge								-	72–76	-	
None (■)	Center	-	0	10–15	30	<10	10–15	-	-	-	-	Moore et al. (2007)
	Edge	-	<10	<10	20	<10	20	-	-	-	-	
	Reference	-	0	<10	20	10–20	30–60	-	-	-	-	
Haida-2000a (■)	Center	6.0–6.8	1.7–2.7	0.4–0.8	58–62	-	0–12	10–19	20	20	60	Peterson (2005); Peterson et al. (2011)
	Edge	7.2–7.3	0	2.3–3.0	42–47	-	3.2–15	15–22	5	15	80	
	Reference	6.5–8.7	0–2.9	0	42–46	-	4.8–8.6	15–20	5	15	80	
None (●)	Center	-	628 ± 225	-	-	2.65×10^{13}	1.56×10^{11}	-	-	-	-	Guidi et al. (2012)
	Edge	-	335 ± 130	-	-	2.38×10^{13}	1.41×10^{11}	-	-	-	-	
ACE1	Center	0.39 ± 0.32(2.5)	0.52 ± 0.39(3.3)	5.29 ± 1.01(34)	1.47 ± 0.28(9.4)	4.37 ± 0.84(28)	3.58 ± 0.47(23)	0.01 ± 0.01(0.1)	6	43	51	This study
ACE2	Edge	0.43 ± 0.13(2.1)	1.39 ± 0.62(6.7)	8.51 ± 0.93(41)	1.83 ± 0.14(8.8)	4.76 ± 0.97(23)	3.35 ± 0.70(16)	0.26 ± 0.30(1.2)	9	51	40	
ACE3	Reference	0.33 ± 0.17(2.5)	0.56 ± 0.17(4.3)	3.91 ± 1.64(30)	1.28 ± 0.57(9.8)	3.37 ± 0.79(26)	3.32 ± 0.76(25)	0.16 ± 0.24(1.2)	7	40	53	

Note. The symbols were used to classify the methods for phytoplankton biomass representation. ▲: Cell counting by microscope (cell/L^1); ■: HPLC-pigments divided by TChl *a* (relative units); ●: flow cytometry (cell/m^2), except fucoxanthin concentration for diatoms (μg/m^2). The values for the present study were upper 100-m inventory (mg/m^2) with the percentage inside the parentheses. The data of Haida-2000a were only for the September 2000 cruise and were accessed from (Peterson, 2005) and Peterson et al. (2011). Dino- = dinoflagellates, Diat- = diatoms, Hapto-8 = haptophyte-8, Hapto-6 = haptophyte-6, *Proc* = *Prochlorococcus*, *Syne* = *Synechococcus*, Pras = prasinophytes; ACE = anticyclonic eddy; HPLC = high-performance liquid chromatography.

is consistent with the pattern in Haida-2000a (Peterson et al., 2011), in which ~80% of the carbon biomass was accounted for by pennate diatoms at the center or edge, although the contributions of diatoms to cell abundance and fucoxanthin concentration were not as high. Notably, the Si $(OH)_4$ concentration was in excess in the upper 50 m at the center and edge, in contrast to the depleted Si $(OH)_4$ concentrations at the reference. The analysis also implied that DIN was the principal limiting nutrient. In our study, DIN was almost exhausted in the upper 50 m. The nutricline was at ~100 m at the center or reference, so that DIN was scarce in the entire euphotic zone. At the edge, nutrients could be supplied by nutrient pumping, and the nutricline was at ~50 m. It was easy to understand the increasing diatom biomass at the edge, where nutrient pumping generated by upwelling could mitigate the effect of the higher half-saturation constant (K_s = 0.7–1 μM) of some diatom species (Eppley et al., 1969).

The response of the pico-phytoplankton, *Prochlorococcus* and *Synechococcus*, was different. First, although the TChl *a* concentrations were very similar at the center and edge, *Prochlorococcus* contributed ~37% and 18% of the elevated TChl *a* concentrations, respectively, relative to the reference. There have been some reports of a positive response of *Prochlorococcus* to ACEs (Baltar et al., 2010; Fernández et al., 2008; Girault et al., 2013; Lasternas et al., 2013), presumably because *Prochlorococcus* benefits from the warmer, oligotrophic water in ACEs (Agawin et al., 2000). The enhancement of the *Prochlorococcus* Chl *a* concentration is dramatic considering the higher cell mortality and lysis rates at the centers of ACEs (Lasternas et al., 2013). Second, there was no difference in the *Synechococcus* Chl *a* concentration inventory among all stations in our study: *Synechococcus* was distributed principally in the upper 50 m of the water column. This pattern was explained by their preference for high irradiance compared to the adaptation of *Prochlorococcus* to low light (Moore et al., 1995; Partensky et al., 1999). However, in our study, the most extreme environmental gradients were accompanied by depressed isopycnals, which in general extended deeper than 50 m. Because of its requirement of high light intensity, *Synechococcus* resides mainly in the water near the surface. A depression of isopycnals deepens the upper mixed layer, and this deepening might be responsible for the homogeneous distribution of *Synechococcus* Chl *a* concentrations.

4.3. Higher TChl *a* Concentration at the Edge but More Particle Export at the Center of the ACEs—Was Vertical-Lateral Transport Coupled With the Community Composition?

Phytoplankton are the major component of POC in marine ecosystems (Laws et al., 1988; Michaels & Silver, 1988), although bacterial biomass may contribute ~40% to the POC in oligotrophic water (Cho & Azam, 1990). Therefore, variations in phytoplankton biomass and community succession can affect the POC stock and POC flux to a great extent through mechanisms such as sinking of dead cells, sinking of cell aggregations, and excretion of undigested cells (Boyd & Newton, 1999). In our study, there was a positive correlation overall between POC flux and the TChl *a* inventory in the upper 100 m (Figure 9a). The microphytoplankton and nano-phytoplankton fractions were not related significantly with POC flux, except at the center and edge, respectively (Figures 9b and 9c). Nevertheless, a positive correlation between POC flux and pico-phytoplankton Chl *a* concentration was apparent holistically (Figure 9d). The POC flux was also positively correlated with the *Prochlorococcus* Chl *a* concentration overall (Figure 9f). As mentioned above, the enhancement of the *Prochlorococcus* Chl *a* concentration was remarkable at the center and edge relative to the reference, and, in addition, its contribution to TChl *a* was slightly higher at the edge (~28%) than at the center (~23%). Thus, the gradient of the *Prochlorococcus* Chl *a* concentrations was qualitatively similar to the gradients of the POC fluxes and TChl *a* concentrations (Figure 9a) from the reference through the edge and to the center.

Based on an analysis of data from the same cruise, Zhou et al. (2013) have reported a significant enhancement of particle export in the three eddies estimated from ^{234}Th-derived POC fluxes and the use of both a one-dimensional steady state model (1-D SS model) and a three-dimensional model (3-D model). In the 1-D SS model, the ^{234}Th flux and POC flux at the center were 1.9 and 1.6 times, respectively, the fluxes at the reference. The high POC concentration (stimulated by the upwelling at the eddy edges) induced an increase of particle export. Zhou et al. (2013) therefore introduced a 3-D model to assess and explain the increasing POC flux at the eddy center. Given that the lateral transport velocity was 0.03 m/s and the distance from the edge to the center was 60 km, the lateral flux of ^{234}Th flux was 506 ± 250 dpm·m^{-2}·day^{-1}, which is half that of the ^{234}Th flux observed at the eddy center (1007 ± 29 dpm·m^{-2}·day^{-1}) and almost equal to the ^{234}Th flux at the reference (535 ± 53·dpm·m^{-2}·day^{-1}). A revaluation with the 3-D model revealed that the

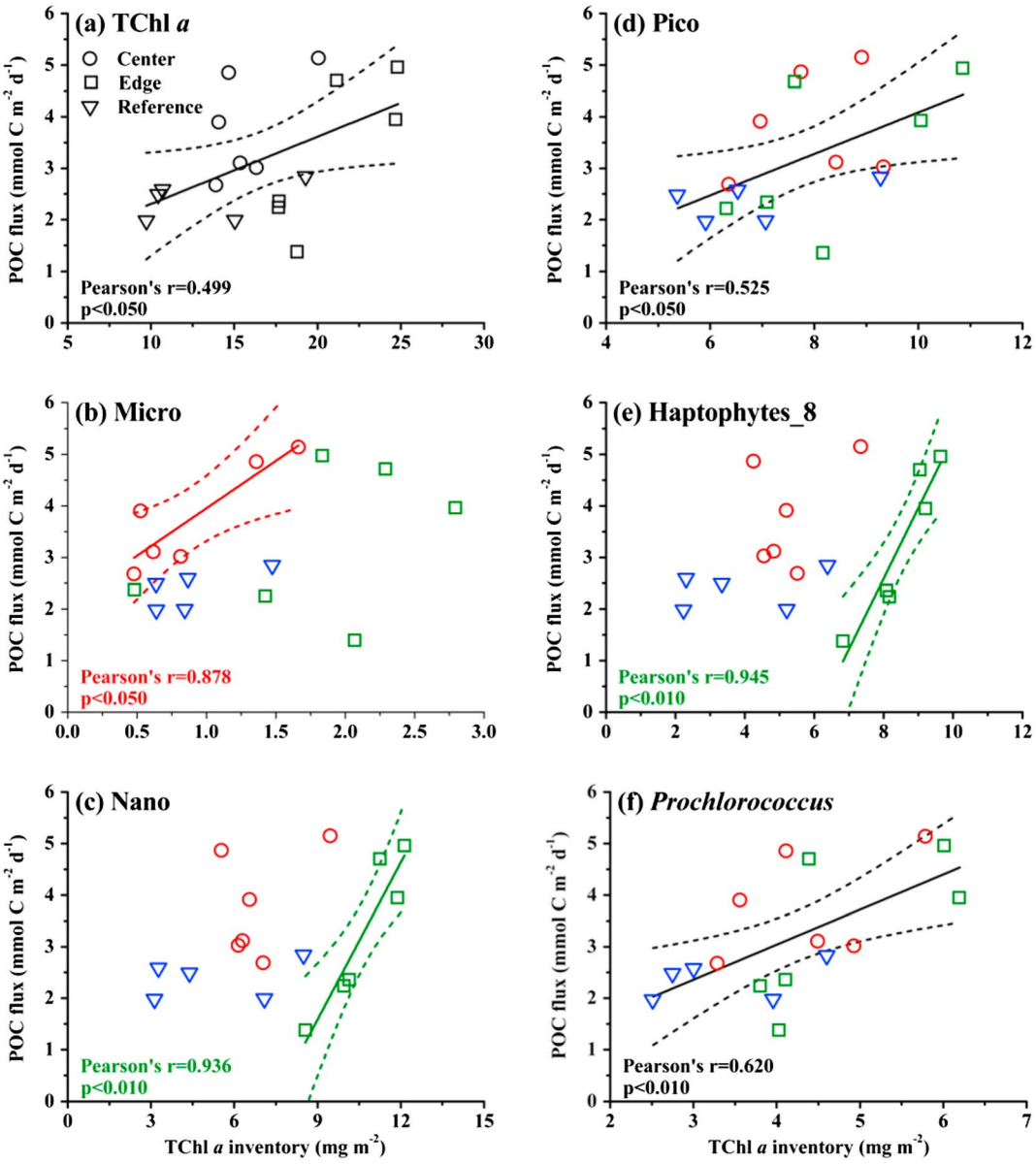

Figure 9. The correlation analysis between POC flux (mmol C·m^{-2}·d^{-1}) and (a) upper 100-m TChl *a* inventory (mg/m^2), (b) microphytoplankton, (c) nano-phytoplankton, (d) pico-phytoplankton, (e) haptophyte-8, and (f) *Prochlorococcus*. The red dots, green squares, and blue inverted triangles represent the ACEs' center, edge, and reference stations, respectively. The linear regression is shown in the same color as the scatters and is in black as the holistic regression. The two dashed lines represent the 95% upper confidence limit and the lower confidence limit. POC = particulate organic carbon; ACES = anticyclonic eddies.

average integrated ^{234}Th flux at the center and edge was 938 ± 284 dpm·m^{-2}·day^{-1} (or POC flux of 3.69 mmol C·m^{-2}·day^{-1}), which was still 1.6 times the flux at the reference.

At the edge, the positive correlation between POC flux and haptophyte-8 was highly significant ($p < 0.01$, Figure 9e). The fact that the TChl *a* concentration at the edge was 2.2 times the concentration at the reference could have affected the POC flux profoundly. Our results were comparable to the positive correlation between haptophyte biomass and POC flux (based on sediment trap data) in the Gulf of Mexico (Hung et al., 2010). The size-fractionated POC/^{234}Th ratios and pigment analyses implied that haptophytes can aggregate into larger particles (up to 20 μm in size) with a relatively high density and rapid sinking rate. However, at the Bermuda Atlantic Time Series site, there is no correlation between

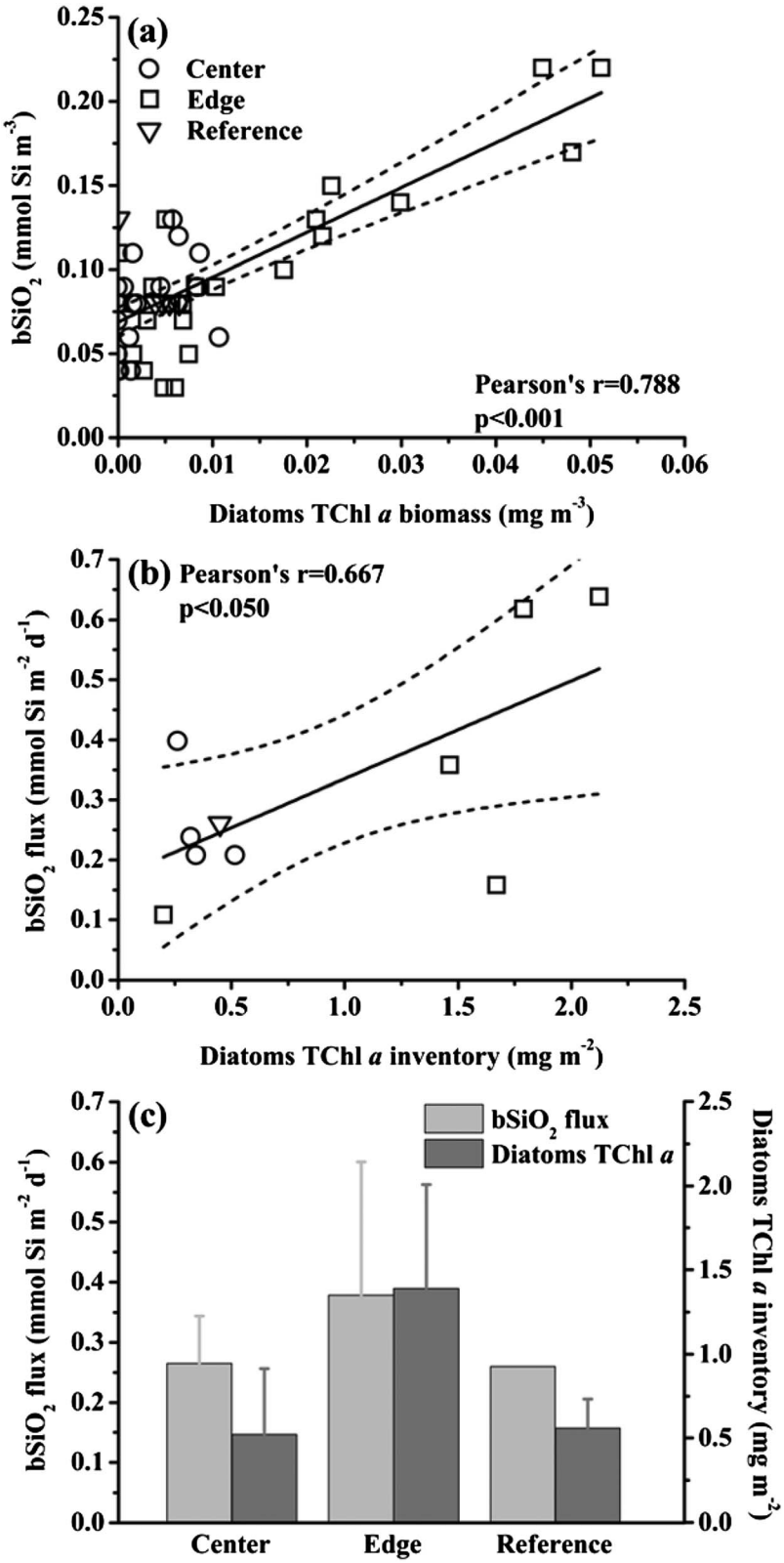

Figure 10. The correlation analysis between (a) $bSiO_2$ concentration (mmol Si/m^3) and diatom TChl *a* concentration (mg/m^3), (b) $bSiO_2$ flux (mmol $Si{\cdot}m^{-2}{\cdot}d^{-1}$) and diatom TChl *a* concentration inventory (mg/m^2), and (c) the histogram of $bSiO_2$ flux and diatom TChl *a* concentration at the ACEs' center, edge, and reference stations. The dots, squares, and inverted triangles represent the center, edge, and reference stations. The linear regression is in the solid line with two dashed lines showing the confidence limits. ACES = anticyclonic eddies.

their Chl *a* concentration and the POC flux, even though haptophytes contribute 25–46% of the TChl *a* concentration (Lomas & Bates, 2004). Interestingly in their study, the POC flux/primary production ratio 8 was significantly correlated in a negative way with the haptophyte Chl *a* concentration, as was the 9 dissolved organic carbon inventory. These correlations imply that heterotrophic activity or recycling processes may hinder the efficiency of the haptophyte-related biological pump. However, in our study, the haptophyte-8 group was the most abundant phytoplankton group and had a profound impact on the carbon cycle, especially at the edge of the ACEs. The species *Dicrateria inornata*, *Imantonia rotunda*, and *Phaeocystis* are included in the haptophytes-8 group, and they are usually the dominant phytoplankton species in the DCML in oligotrophic oceanic water (Alexander et al., 2015).

After combining our results with those of the 1-D model of Zhou et al. (2013), we found that there was a correspondence between the model and data with respect to the enhancement of the TChl *a* concentration and ^{234}Th flux. Both the model and data showed a ~60% elevation of the flux and TChl *a* concentration at the edge relative to the reference. However, the mismatch at the center was striking; the enhancement of the ^{234}Th flux was ~90% compared to only a ~20% increase of the TChl *a* concentration. A comparison of these values at the edge and the center was even more perplexing because the ^{234}Th flux was ~18% higher at the center than at the edge, but there was a ~33% higher TChl *a* concentration at the edge than at the center. To clarify why there was a higher particle export at the center of the ACEs, Zhou et al. (2013) introduced a 3-D model and found that ~50% of the flux at the center was derived from lateral transport of particles from the edge of the ACEs. Because we found a significant positive correlation between POC flux and microphytoplankton Chl *a* concentration at the center (Figure 9b), we hypothesized that some diatoms were transported from the edge to the center and played a leading role in particle export.

The $bSiO_2$ concentration was positively correlated with the diatom Chl *a* concentration at the edge (Figure 10a), and the $bSiO_2$ flux was correlated with the diatom Chl *a* concentration inventory in the upper 100 m (Figure 10b). If the $bSiO_2$ flux was normalized by the diatom Chl *a* concentration, the ratio at the edge was approximately 0.272 mmol Si·mg^{-1} Chl *a*·day^{-1}; the corresponding value at the center was 0.508 mmol Si·mg^{-1} Chl *a*·day^{-1} (Figure 10c), almost double the value at the edge. There was only one $bSiO_2$ flux measurement at the reference, and therefore, it was not included in the comparison. This result was consistent with the results of the 3-D model of Zhou et al. (2013) and implied that ~50% of the sinking diatoms at the center had only a skeleton without pigments and were probably transported laterally from the edge. It is regrettable that we did not have diatom species composition data and meso-zooplankton grazing rate data. Without that information, it is hard to quantify the biomass of diatoms that were transported from ACEs' edge to the center. Lasternas et al. (2013) have found that the mortality of diatoms is ~60% of the diatom cell abundance in an ACE as result of nutrient removal by downwelling. The implication is that the diatoms that were transported laterally suffered from diminishing nutrient availability during their journey from the edge to the center. The mortality of the diatom cells was inevitable, and their frustules were removed from the euphotic zone at the center.

Unlike diatoms, pico-phytoplankton can grow continuously during their lateral movement by taking advantage of their lower nutrient requirements and lower mortality (Baltar et al., 2010; Lasternas et al., 2013). Although it might take 3 weeks or longer to cover the distance from the edge to the center, some living cells could reach the center, especially *Prochlorococcus*. These groups of phytoplankton might sustain 50% of the POC flux at the center, and this might be another explanation for the correlation between the POC flux and haptophyte-8 abundance only at the edge, but for the POC flux and *Prochlorococcus* to be correlated throughout the entire region.

5. Conclusions

This study focused on the impact of three long-lived ACEs on the phytoplankton TChl *a* concentration, community composition, and biogeochemical processes in the northern SCS. The phytoplankton TChl *a* concentrations and community composition were very similar among the three ACEs. However, there were significant differences in the individual spatial division, TChl *a* concentration, and community composition among the center, edge, and reference stations of the ACEs. Higher TChl *a* concentrations at the edge stations were attributed to increasing contributions to TChl *a* from haptophyte-8, *Prochlorococcus*, and diatoms, and they could be explained by nutrient pumping at the edge.

Synechococcus was distributed on depressed isopycnals and showed only a slight response to the ACEs, both at the center and at the edge.

The relationship between phytoplankton TChl *a* concentrations and POC fluxes implied that both TChl *a* concentrations3 and community composition had an impact on particle export. Based on the 1-D and 3-D models described by Zhou et al. (2013), the phenomenon of higher TChl *a* concentrations at the eddy edge but higher export at the center might be explained by a combination of vertical convection and lateral transport. The lateral transport of diatoms might explain the ~50% enhancement in $bSiO_2$ flux at the core. In addition, the significant positive correlation between the POC flux and haptophyte-8 Chl *a* concentration at the edge implied an important role of haptophyte-8 in the biogeochemical cycle, and the overall positive correlation between POC flux and *Prochlorococcus* was evidence of the significance of lateral transport, especially for the phytoplankton groups adapted to low nutrient concentrations.

Acknowledgments

This study was funded by grants from the National Key R&D Program of China (2016YFA0601201) and the Natural Science Foundation of China through grants 41330961, 4173000226 and 41776146. All of the pigment data and CHEMTAX results could be acquired from the supporting information and please contact Huang (bqhuang@xmu.edu.cn) if any questions. And the POC fluxes data could be acquired from the supporting information of Zhou et al. (2013) (https://doi.org/10.1016/j.epsl.2013.07.039). We thank the Captain and Crew of R/V *Dongfanghong 2* for their assistance in the sampling during the cruise. We appreciate the sharing of the CTD data by Jiwei Tian of the Ocean University of China. We are also grateful to the measurements and analyses of nutrients by Aiqin Han. We thank Kuo-ping Chiang for the suggestions during preparation of the manuscript. We are also grateful for the graphic processing software of Ocean Data View (version 4.5.7, contributed by Schlitzer, R., http://odv.awi.de, 2013) and OriginPro 8.5 (OriginLab Corporation©, Northampton, MA 01060 USA). Finally, we thank John Hodgkiss of the University of Hong Kong for his help with English editing.

References

Agawin, N. S. R., Duarte, C. M., & Agustí, S. (2000). Nutrient and temperature control of the contribution of picoplankton to phytoplankton biomass and production. *Limnology and Oceanography*, *45*(3), 591–600. https://doi.org/10.4319/lo.2000.45.3.0591

Alexander, H., Rouco, M., Haley, S. T., Wilson, S. T., Karl, D. M., & Dyhrman, S. T. (2015). Functional group-specific traits drive phytoplankton dynamics in the oligotrophic ocean. *Proceedings of the National Academy of Sciences of the United States of America*, *112*(44), E5972–E5979. https://doi.org/10.1073/pnas.1518165112

Baltar, F., Arístegui, J., Gasol, J. M., Lekunberri, I., & Herndl, G. J. (2010). Mesoscale eddies: 10 hotspots of prokaryotic activity and differential community structure in the ocean. *The ISME Journal*, *4*(8), 975–988. https://doi.org/10.1038/ismej.2010.33

Biggs, D. C. (1992). Nutrients, plankton, and productivity in a warm-core ring in the western Gulf of Mexico. *Journal of Geophysical Research*, *97*(C2), 2143–2154. https://doi.org/10.1029/90JC02020

Boyd, P. W., & Newton, P. P. (1999). Does planktonic community structure determine downward particulate organic carbon flux in different oceanic provinces? *Deep-Sea Research Part I: Oceanographic Research Papers*, *46*(1), 63–91. https://doi.org/10.1016/S0967-0637(98)00066-1

Campbell, R., Diaz, F., Hu, Z., Doglioli, A., Petrenko, A., & Dekeyser, I. (2013). Nutrients and plankton spatial distributions induced by a coastal eddy in the Gulf of Lion. Insights from a numerical model. *Progress in Oceanography*, *109*, 47–69. https://doi.org/10.1016/j.pocean.2012.09.005

Chelton, D. B., Schlax, M. G., & Samelson, R. M. (2011). Global observations of nonlinear mesoscale eddies. *Progress in Oceanography*, *91*(2), 167–216. https://doi.org/10.1016/j.pocean.2011.01.002

Cho, B. C., & Azam, F. (1990). Biogeochemical significance of bacterial biomass in the ocean's euphotic zone. *Marine Ecology Progress Series*, *63*, 253–259. https://doi.org/10.3354/meps063253

Crawford, W. R., Brickley, P. J., & Thomas, A. C. (2007). Mesoscale eddies dominate surface phytoplankton in the northern Gulf of Alaska. *Progress in Oceanography*, *75*(2), 287–303. https://doi.org/10.1016/j.pocean.2007.08.016

Dietze, H., Matear, R., & Moore, T. (2009). Nutrient supply to anticyclonic meso-scale eddies off western Australia estimated with artificial tracers released in a circulation model. *Deep-Sea Research Part I: Oceanographic Research Papers*, *56*(9), 1440–1448. https://doi.org/10.1016/j.dsr.2009.04.012

Eden, C., & Dietze, H. (2009). Effects of mesoscale eddy/wind interactions on biological new production and eddy kinetic energy. *Journal of Geophysical Research*, *114*, C05023. https://doi.org/10.1029/2008JC005129

Eppley, R. W., Rogers, J. N., & McCarthy, J. J. (1969). Half-saturation constants for uptake of nitrate and ammonium by marine phytoplankton. *Limnology and Oceanography*, *14*(6), 912–920. https://doi.org/10.4319/lo.1969.14.6.0912

Fernández, C., Thyssen, M., & Denis, M. (2008). Microbial community structure along 18°W (39°N–44.5°N) in the NE Atlantic in late summer 2001 (POMME programme). *Journal of Marine Systems*, *71*(1–2), 46–62. https://doi.org/10.1016/j.jmarsys.2007.06.003

Flierl, G. R., & Mied, R. P. (1985). Frictionally induced circulations and spin down of a warm core ring. *Journal of Geophysical Research*, *90*(C5), 8917–8927. https://doi.org/10.1029/JC090iC05p08917

Fong, A. A., Karl, D. M., Lukas, R., Letelier, R. M., Zehr, J. P., & Church, M. J. (2008). Nitrogen fixation in an anticyclonic eddy in the oligotrophic north Pacific Ocean. *The ISME Journal*, *2*(6), 663–676. https://doi.org/10.1038/ismej.2008.22

Franks, P. J. S., Wroblewski, J. S., & Flierl, G. R. (1986). Prediction of phytoplankton growth in response to the frictional decay of a warm-core ring. *Journal of Geophysical Research*, *91*(C6), 7603–7610. https://doi.org/10.1029/JC091iC06p07603

Furuya, K., Hayashi, M., & Yabushita, Y. (1998). HPLC determination of phytoplankton pigments using N,N-Dimethylformamide. *Journal of Oceanography*, *54*(2), 199–203. https://doi.org/10.1007/BF02751695

Girault, M., Arakawa, H., Barani, A., Ceccaldi, H. J., Hashihama, F., Kinouchi, S., & Gregori, G. (2013). Distribution of ultraphytoplankton in the western part of the North Pacific subtropical gyre during a strong La Niña condition: Relationship with the hydrological conditions. *Biogeosciences*, *10*(9), 5947–5965. https://doi.org/10.5194/bg-10-5947-2013

Glover, D. M., Doney, S. C., Nelson, N. B., & Wallis, A. (2008). Submesoscale anisotropy (fronts, eddies, and filaments) as observed near Bermuda with ocean color data. in *Ocean Science Meeting*. edited by O. presentation. Orlando.

Guidi, L., Calil, P. H. R., Duhamel, S., Björkman, K. M., Doney, S. C., Jackson, G. A., et al. (2012). Does eddy-eddy interaction control surface phytoplankton distribution and carbon export in the North Pacific subtropical gyre? *Journal of Geophysical Research*, *117*, G02024. https://doi.org/10.1029/2012JG001984

Hansen, C., Kvaleberg, E., & Samuelsen, A. (2010). Anticyclonic eddies in the Norwegian Sea; their generation, evolution and impact on primary production. *Deep-Sea Research Part I: Oceanographic Research Papers*, *57*(9), 1079–1091. https://doi.org/10.1016/j.dsr.2010.05.013

Huang, B., Hu, J., Xu, H., Cao, Z., & Wang, D. (2010). Phytoplankton community at warm eddies in the northern South China Sea in winter 2003/2004. *Deep Sea Research Part II: Topical Studies in Oceanography*, *57*(19–20), 1792–1798. https://doi.org/10.1016/j.dsr2.2010.04.005

Hung, C.-C., Xu, C., Santschi, P. H., Zhang, S.-J., Schwehr, K. A., Quigg, A., et al. (2010). Comparative evaluation of sediment trap and ^{234}Th-derived POC fluxes from the upper oligotrophic waters of the Gulf of Mexico and the subtropical northwestern Pacific Ocean. *Marine Chemistry*, *121*(1–4), 132–144. https://doi.org/10.1016/j.marchem.2010.03.011

Hwang, C., & Chen, S.-A. (2000). Circulations and eddies over the South China Sea derived from TOPEX/Poseidon altimetry. *Journal of Geophysical Research*, *105*(C10), 23,943–23,965. https://doi.org/10.1029/2000JC900092

Jeffrey, S. W., & Hallegraeff, G. M. (1980). Studies of phytoplankton species and photosynthetic pigments in a warm core eddy of the east Australian Current. I. Summer populations. *Marine Ecology Progress Series*, *3*, 285–294. https://doi.org/10.3354/meps003285

José, Y. S., Aumont, O., Machu, E., Penven, P., Moloney, C. L., & Maury, O. (2014). Influence of mesoscale eddies on biological production in the Mozambique channel: Several contrasted examples from a coupled ocean-biogeochemistry model. *Deep Sea Research Part II: Topical Studies in Oceanography*, *100*, 79–93. https://doi.org/10.1016/j.dsr2.2013.10.018

Kim, D., Yang, E. J., Kim, K. H., Shin, C.-W., Park, J., Yoo, S., & Hyun, J.-H. (2012). Impact of an anticyclonic eddy on the summer nutrient and chlorophyll a distributions in the Ulleung Basin, East Sea (Japan Sea). *ICES Journal of Marine Science*, *69*(1), 23. https://doi.org/10.1093/icesjms/fsr178–29

Kishi, M. J. (1994). Prediction of phytoplankton growth in a warm-core ring using three dimensional ecosystem model. *Journal of Oceanography*, *50*(5), 489–498. https://doi.org/10.1007/BF02235419

Klein, P., & Lapeyre, G. (2009). The oceanic vertical pump induced by mesoscale and submesoscale turbulence. *Annual Review of Marine Science*, *1*(1), 351–375. https://doi.org/10.1146/annurev.marine.010908.163704

Kolber, Z. S. (2006). Getting a better picture of the ocean's nitrogen budget. *Science*, *312*(5779), 1479–1480. https://doi.org/10.1126/science.1129129

Landry, M. R., Brown, S. L., Rii, Y. M., Selph, K. E., Bidigare, R. R., Yang, E. J., & Simmons, M. P. (2008). Depth-stratified phytoplankton dynamics in Cyclone Opal, a subtropical mesoscale eddy. *Deep Sea Research Part II: Topical Studies in Oceanography*, *55*(10-13), 1348–1359. https://doi.org/10.1016/j.dsr2.2008.02.001

Lasternas, S., Piedeleu, M., Sangrà, P., Duarte, C. M., & Agustí, S. (2013). Forcing of dissolved organic carbon release by phytoplankton by anticyclonic mesoscale eddies in the subtropical NE Atlantic Ocean. *Biogeosciences*, *10*(3), 2129–2143. https://doi.org/10.5194/bg-10-2129-2013

Latasa, M. (2007). Improving estimations of phytoplankton class abundances using CHEMTAX. *Marine Ecology Progress Series*, *329*, 13–21. https://doi.org/10.3354/meps329013

Laws, E. A., Bienfang, P. K., Ziemann, D. A., & Conquest, L. D. (1988). Phytoplankton population dynamics and the fate of production during the spring bloom in Auke Bay, Alaska. *Limnology and Oceanography*, *33*(1), 57–67. https://doi.org/10.4319/lo.1988.33.1.0057

Leterme, S. C., & Pingree, R. D. (2008). The Gulf Stream, rings and North Atlantic eddy structures from remote sensing (altimeter and SeaWiFS). *Journal of Marine Systems*, *69*(3-4), 177–190. https://doi.org/10.1016/j.jmarsys.2005.11.022

Lévy, M., Klein, P., & Jelloul, M. B. (2009). New production stimulated by high-frequency winds in a turbulent mesoscale eddy field. *Geophysical Research Letters*, *36*, L16603. https://doi.org/10.1029/2009GL039490

Lévy, M., Klein, P., & Treguier, A.-M. (2001). Impact of sub-mesoscale physics on production and subduction of phytoplankton in an oligotrophic regime. *Journal of Marine Research*, *59*(4), 535–565. https://doi.org/10.1357/002224001762842181

Lin, I.-I., Lien, C. C., Wu, C. R., Wong, G. T. F., Huang, C. W., & Chiang, T. L. (2010). Enhanced primary production in the oligotrophic South China Sea by eddy injection in spring. *Geophysical Research Letters*, *37*, L16602. https://doi.org/10.1029/2010GL043872

Liu, F., Tang, S., & Chen, C. (2013). Impact of nonlinear mesoscale eddy on phytoplankton distribution in the northern South China Sea. *Journal of Marine Systems*, *123-124*, 33–40. https://doi.org/10.1016/j.jmarsys.2013.04.005

Lomas, M. W., & Bates, N. R. (2004). Potential controls on interannual partitioning of organic carbon during the winter/spring phytoplankton bloom at the Bermuda Atlantic time-series study (BATS) site. *Deep-Sea Research Part I: Oceanographic Research Papers*, *51*(11), 1619–1636. https://doi.org/10.1016/j.dsr.2004.06.007

MacFadyen, A., Hickey, B. M., & Cochlan, W. P. (2008). Influences of the Juan de Fuca eddy on circulation, nutrients, and phytoplankton production in the northern California Current System. *Journal of Geophysical Research*, *113*, C08008. https://doi.org/10.1029/2007JC004412

Mackey, M. D., Mackey, D. J., Higgins, H. W., & Wright, S. W. (1996). CHEMTAX—a program for estimating class abundances from chemical markers: Application to HPLC measurements of phytoplankton. *Marine Ecology Progress Series*, *144*, 265–283. https://doi.org/10.3354/meps144265

Mahadevan, A., & Archer, D. (2000). Modeling the impact of fronts and mesoscale circulation on the nutrient supply and biogeochemistry of the upper ocean. *Journal of Geophysical Research*, *105*(C1), 1209–1225. https://doi.org/10.1029/1999JC900216

Martin, A. P., & Pondaven, P. (2003). On estimates for the vertical nitrate flux due to eddy pumping. *Journal of Geophysical Research*, *108*(C11), 3359. https://doi.org/10.1029/2003JC001841

Martin, A. P., & Richards, K. J. (2001). Mechanisms for vertical nutrient transport within a North Atlantic mesoscale eddy. *Deep Sea Research Part II: Topical Studies in Oceanography*, *48*(4–5), 757–773. https://doi.org/10.1016/S0967-0645(00)00096-5

McGillicuddy, D. J., Anderson, L. A., Bates, N. R., Bibby, T., Buesseler, K. O., Carlson, C. A., et al. (2007). Eddy/wind interactions stimulate extraordinary mid-Ocean plankton blooms. *Science*, *316*(5827), 1021–1026. https://doi.org/10.1126/science.1136256

McGillicuddy, D. J., Anderson, L. A., Doney, S. C., & Maltrud, M. E. (2003). Eddy-driven sources and sinks of nutrients in the upper ocean: Results from a 0.1° resolution model of the North Atlantic. *Global Biogeochemical Cycles*, *17*(2), 1035. https://doi.org/10.1029/2002GB001987

McGillicuddy, D. J., Robinson, A. R., Siegel, D. A., Michaels, A. F., Bates, N. R., & Knap, A. H. (1999). Mesoscale variations of biogeochemical properties in the Sargasso Sea. *Journal of Geophysical Research*, *104*(C6), 13,381–13,394. https://doi.org/10.1029/1999JC900021

Michaels, A. F., & Silver, M. W. (1988). Primary production, sinking fluxes and the microbial food web. *Deep-Sea Research Part A: Oceanographic Research Papers*, *35*(4), 473–490. https://doi.org/10.1016/0198-0149(88)90126-4

Moore, L. R., Goericke, R., & Chisholm, S. W. (1995). Comparative physiology of *Synechococcus* and *Prochlorococcus*: Influence of light and temperature on growth, pigments, fluorescence and absorptive properties. *Marine Ecology Progress Series*, *116*, 259–275. https://doi.org/10.3354/meps116259

Moore, T. S., Mateara, R. J., Marrac, J., & Clementson, L. (2007). Phytoplankton variability off the western Australian coast: Mesoscale eddies and their role in cross-shelf exchange. *Deep Sea Research Part II: Topical Studies in Oceanography*, *54*(8-10), 943–960. https://doi.org/10.1016/j.dsr2.2007.02.006

Nan, F., He, Z., Zhou, H., & Wang, D. (2011). Three long-lived anticyclonic eddies in the northern South China Sea. *Journal of Geophysical Research*, *116*, C05002. https://doi.org/10.1029/2010JC006790

Nelson, D. M., McCarthy, J. J., Joyce, T. M., & Ducklow, H. W. (1989). Enhanced near-surface nutrient availability and new production resulting from the frictional decay of a Gulf Stream warm-core ring. *Deep-Sea Research Part A: Oceanographic Research Papers*, *36*(5), 705–714. https://doi.org/10.1016/0198-0149(89)90146-5

Ning, X., Chai, F., Xue, H., Cai, Y., Liu, C., & Shi, J. (2004). Physical-biological oceanographic coupling influencing phytoplankton and primary production in the South China Sea. *Journal of Geophysical Research*, *109*, C10005. https://doi.org/10.1029/2004JC002365

Ning, X., Peng, X., Le, F., Hao, Q., Sun, J., Liu, C., & Cai, Y. (2008). Nutrient limitation of phytoplankton in anticyclonic eddies of the northern South China Sea. *Biogeosciences Discussions*, *5*(6), 4591–4619. https://doi.org/10.5194/bgd-5-4591-2008

Nurser, A. J. G., & Zhang, J. W. (2000). Eddy-induced mixed layer shallowing and mixed layer/thermocline exchange. *Journal of Geophysical Research*, *105*(C9), 21,851–21,868. https://doi.org/10.1029/2000JC900018

Oguz, T., & Salihoglu, B. (2000). Simulation of eddy-driven phytoplankton production in the Black Sea. *Geophysical Research Letters*, *27*(14), 2125–2128. https://doi.org/10.1029/1999GL011083

Omand, M. M., D'Asaro, E. A., Lee, C. M., Perry, M. J., Briggs, N., Cetinić, I., & Mahadevan, A. (2015). Eddy-driven subduction exports particulate organic carbon from the spring bloom. *Science*, *348*(6231), 222–225. https://doi.org/10.1126/science.1260062

Oschlies, A., & Garçon, V. (1998). Eddy-induced enhancement of primary production in a model of the north Atlantic Ocean. *Nature*, *394*(6690), 266–269. https://doi.org/10.1038/28373

Painter, S. C., Pidcock, R. E., & Allen, J. (2010). A mesoscale eddy driving spatial and temporal heterogeneity in the productivity of the euphotic zone of the northeast Atlantic. *Deep Sea Research Part II: Topical Studies in Oceanography*, *57*(15), 1281–1292. https://doi.org/10.1016/j.dsr2.2010.01.005

Partensky, F., Blanchot, J., & Vaulot, D. (1999). Differential distribution of *Prochlorococcus* and *Synechococcus* in oceanic waters: A review. in *Marine cyanobacteria and related organisms*. edited by L. Charpy and A. W. D. Larkum. pp. 457–475. Bulletin de l'Institut océanographique. Monaco.

Paterson, H. L., Feng, M., Waite, A. M., Gomis, D., Beckley, L. E., Holliday, D., & Thompson, P. A. (2008). Physical and chemical signatures of a developing anticyclonic eddy in the Leeuwin Current, eastern Indian Ocean. *Journal of Geophysical Research*, *113*, C07049. https://doi.org/10.1029/2007JC004707

Perissinotto, R., & Rae, C. M. D. (1990). Occurrence of anticyclonic eddies on the Prince Edward plateau (Southern Ocean): Effects on phytoplankton biomass and production. *Deep-Sea Research Part A: Oceanographic Research Papers*, *37*(5), 777–793. https://doi.org/10.1016/0198-0149(90)90006-H

Peterson, T. D. (2005). *Studies on the biological oceanography of Haida eddies*. Vancouver: University of British Columbia.

Peterson, T. D., Crawford, D. W., & Harrison, P. J. (2011). Evolution of the phytoplankton assemblage in a long-lived mesoscale eddy in the eastern Gulf of Alaska. *Marine Ecology Progress Series*, *424*, 53–73. https://doi.org/10.3354/meps08943

Sasai, Y., Sasaki, H., & Richards, K. J. (2013). Impact of physical processes on the phytoplankton blooms in the South China Sea: An eddy-resolving physical-biological model study. *Biogeosciences Discussions*, *10*(1), 1577–1604. https://doi.org/10.5194/bgd-10-1577-2013

Sweeney, E. N., McGillicuddy, D. J., & Buesseler, K. O. (2003). Biogeochemical impacts due to mesoscale eddy activity in the Sargasso Sea as measured at the Bermuda Atlantic time-series study (BATS). *Deep Sea Research Part II: Topical Studies in Oceanography*, *50*(22-26), 3017–3039. https://doi.org/10.1016/j.dsr2.2003.07.008

Tanaka, T., Thingstad, T. F., Christaki, U., Colombet, J., Cornet-Barthaux, V., Courties, C., et al. (2011). Lack of P-limitation of phytoplankton and heterotrophic prokaryotes in surface waters of three anticyclonic eddies in the stratified Mediterranean Sea. *Biogeosciences*, *8*(2), 525–538. https://doi.org/10.5194/bg-8-525-2011

Toner, M., Kirwan, A. D., Poje, A. C., Kantha, L. H., Müller-Karger, F. E., & Jones, C. K. R. T. (2003). Chlorophyll dispersal by eddy-eddy interactions in the Gulf of Mexico. *Journal of Geophysical Research*, *108*(C4), 3105. https://doi.org/10.1029/2002JC001499

Tranter, D. J., Parker, R. R., & Cresswekk, G. R. (1980). Are warm-core eddies unproductive? *Nature*, *284*(5756), 540–542. https://doi.org/10.1038/284540a0

Uitz, J., Claustre, H., Morel, A., & Hooker, S. B. (2006). Vertical distribution of phytoplankton communities in open ocean: An assessment based on surface chlorophyll. *Journal of Geophysical Research*, *111*, C08005. https://doi.org/10.1029/2005JC003207

Waite, A. M., Stemmann, L., Guidi, L., Calil, P. H. R., Hogg, A. M. C., Feng, M., et al. (2016). The wineglass effect shapes particle export to the deep ocean in mesoscale eddies. *Geophysical Research Letters*, *43*, 9791–9800. https://doi.org/10.1002/2015GL066463

Washburn, L., Swenson, M. S., Largier, J. L., Kosro, P. M., & Ramp, S. R. (1993). Cross-shelf sediment transport by an anticyclonic eddy off Northern California. *Science*, *261*(5128), 1560–1564. https://doi.org/10.1126/science.261.5128.1560

Woodward, E. M. S., & Rees, A. P. (2001). Nutrient distributions in an anticyclonic eddy in the northeast Atlantic Ocean, with reference to nanomolar ammonium concentrations. *Deep Sea Research Part II: Topical Studies in Oceanography*, *48*(4–5), 775–793. https://doi.org/10.1016/S0967-0645(00)00097-7

Xiu, P., & Chai, F. (2011). Modeled biogeochemical responses to mesoscale eddies in the South China Sea. *Journal of Geophysical Research*, *116*(C10). https://doi.org/10.1029/2010JC006800

Zapata, M., Jeffrey, S. W., Wright, S. W., Rodríguez, F., Garrido, J. L., & Clementson, L. (2004). Photosynthetic pigments in 37 species (65 strains) of haptophyta: Implications for oceanography and chemotaxonomy. *Marine Ecology Progress Series*, *270*, 83–102. https://doi.org/10.3354/meps270083

Zapata, M., Rodríguez, F., & Garrido, J. L. (2000). Separation of chlorophylls and carotenoids from marine phytoplankton: A new HPLC method using a reversed-phase C8 column and pyridine-containing mobile phases. *Marine Ecology Progress Series*, *195*, 29–45. https://doi.org/10.3354/meps195029

Zhang, J.-Z., Wanninkhof, R., & Lee, K. (2001). Enhanced new production observed from the diurnal cycle of nitrate in an oligotrophic anticyclonic eddy. *Geophysical Research Letters*, *28*(8), 1579–1582. https://doi.org/10.1029/2000GL012065

Zhang, Z., Zhang, Y., Wang, W., & Huang, R. X. (2013). Universal structure of mesoscale eddies in the ocean. *Geophysical Research Letters*, *40*, 3677–3681. https://doi.org/10.1002/grl.50736

Zhou, K., Dai, M., Kao, S.-J., Wang, L., Xiu, P., Chai, F., et al. (2013). Apparent enhancement of ^{234}Th-based particle export associated with anticyclonic eddies. *Earth and Planetary Science Letters*, *381*, 198–209. https://doi.org/10.1016/j.epsl.2013.07.039